

**A novel multilevel boost converter for Fuel Cell applications**

Victor M. Sanchez<sup>1,\*</sup>, Juan M. Ramirez<sup>2</sup>, Antonio Valderrabano<sup>3</sup>, R. Barbosa<sup>1</sup>

<sup>1</sup>Depto. Ingeniería, Universidad de Quintana Roo,  
Blvd. Bahía s/n E. I. Comonfort, 77019, Chetumal, Q. Roo, México.

\*Tel: 98350300, vsanchez@uqroo.mx

<sup>2</sup>CINVESTAV – Unidad Guadalajara, Av. Científica 1145,  
Col, El Bajío, Zapopan, Jal., México

<sup>3</sup>Universidad Panamericana – Campus Guadalajara,  
Calzada Nueva 49, Ciudad Granja, 45010 Zapopan, Jal., México

**ABSTRACT**

Fuel Cells (FCs) technology is one of the most promising options of alternative energy sources due to its high energy efficiency, extremely low indexes of polluting emissions and high power density. FCs can be an ecological solution to the demand of portable power sources. However, without considering their high costs; there are some technological challenges to solve yet. One of them concerns to the voltage magnitude generated by a fuel cell which has a low value so that it has to be elevated in order to feed electrical loads. To solve this issue, power converter topologies based on power transformers are used. However, power transformers increase the cost and size of the power converters. This work proposes a novel topology of a high gain power converter without power transformer. Moreover, the input current of the proposed converter has a low current ripple which contributes to increase the Fuel Cell lifetime as well as exhibits a high efficiency of energy conversion too. Operating principle, analysis and co-simulation results of a 250 W prototype are shown.

## **1. Introduction**

The main challenges in the design of a power conditioning system for FCs, it is to provide a high gain voltage as well as an input current with a low ripple. The DC voltage produced by a fuel cell ranges between 50-100% of their nominal value as well as it has a low magnitude too. Typically, DC-DC converters based on high frequency transformers are commonly used in order to provide a voltage gain. However, power transformers increase the cost and size of the power conditioning stage [1]. On the other hand, when a high level of current ripple is drawn to the FC, it accelerates the aging of the electrodes [2]. Usually, power converter topologies with input inductor are used in order to reduce the FC's current ripple. The input inductor provides a trade-off between input current ripple and the converter dynamic response. To solve these issues, a novel DC-DC converter topology which has a high gain voltage and low ripple at the input current is proposed. The power converter is comprised by an interleaved boost converter cascaded with a voltage multiplier based on a multilevel converter.

Two parallel boost converters integrate the stage of the interleaved boost converter. This arrangement reduces the current stress in the converter switches. The input inductors of each one of the boost converters are coupled and they operate in Discontinuous Current Mode. This strategy is used in order to get a uniform current distribution between each converter, without the requirement of a current sharing control [3].

The multilevel stage provides an additional gain that multiplies the input stage's voltage gain. This converter is based on a multilevel voltage configuration, which multiplies the input voltage as well as it maintains a balance in the voltage of the output capacitors too. Moreover, the voltage gain of this stage is obtained by low voltage switches. Additionally, the multilevel converter provides the following advantages: (i) low harmonic distortion, (ii) low emission of electromagnetic noise, (iii) high efficiency, (iv) not uses power transformers [4].

This paper is organized as follows. Section II describes the power converter topology and it explains the operating principle of the high-gain converter. Section III presents the co-simulation results and finally in section IV the conclusions of this work are presented.

## 2. Multilevel-interleaved boost converter

The topology of the multilevel-interleaved boost converter is shown in Figure 1.

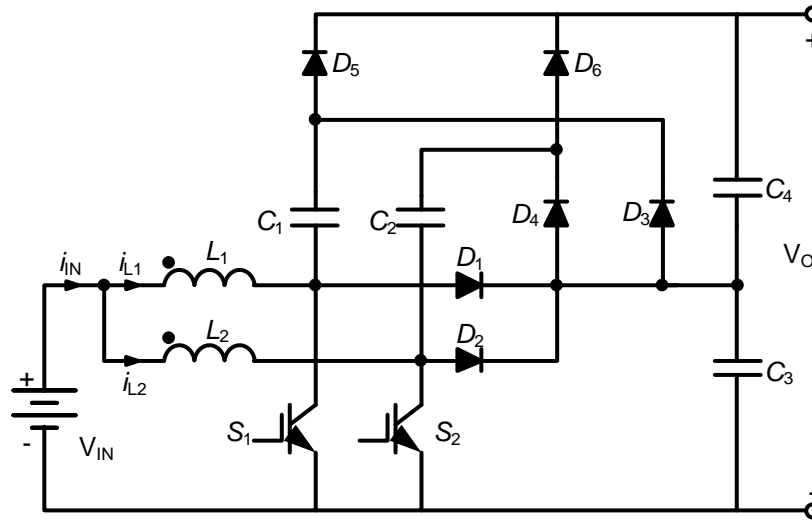


Figure 1. Multilevel-interleaved boost converter.

The converter consists of two DC-DC converters in cascade, as it is described in the block diagram on Figure 2.

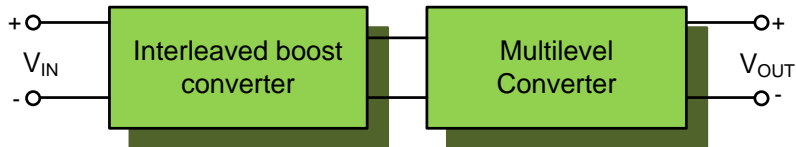


Figure 2. Block diagram of novel power converter.

The DC-DC converter operation can be explained by analyzing separately of both converters, and then by combining their input-output relationships.

### 2.1 Input stage

The interleaved boost converter provides an initial voltage gain as well as it has a low ripple in the input current. The total input current is divided between the two boost converters. The input inductors are magnetically coupled. The coupling of the input inductors allows an equal current sharing in each converter despite of the boost converters'

duty cycle variations. In order to simplify the power converter analysis, the coupling inductors can be represented by an equivalent circuit of three decoupled inductors', as it is showed in Figure 3.

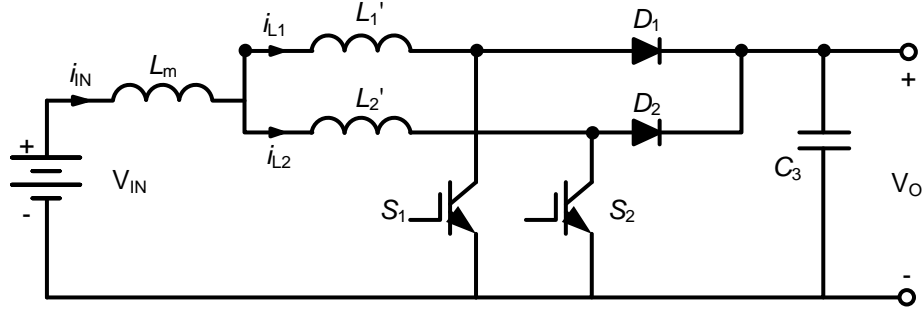


Figure 3. Equivalent circuit of the interleaved boost converter

The relationship between the coupled inductors becomes:

$$L'_1 = L_1 - L_m \quad (1)$$

$$L'_2 = L_2 - L_m \quad (2)$$

$$L_m = k\sqrt{L_1 L_2} \quad (3)$$

Where  $L_1$  and  $L_2$  are the inductance values of the two inductors,  $k$  is the coupling coefficient,  $L'_1$  and  $L'_2$  are the leakage inductances, and  $L_m$  is the mutual inductance.

The interleaved boost converter operation consists of six different switching states. Figure 4 illustrates the equivalent circuits during each switching state.

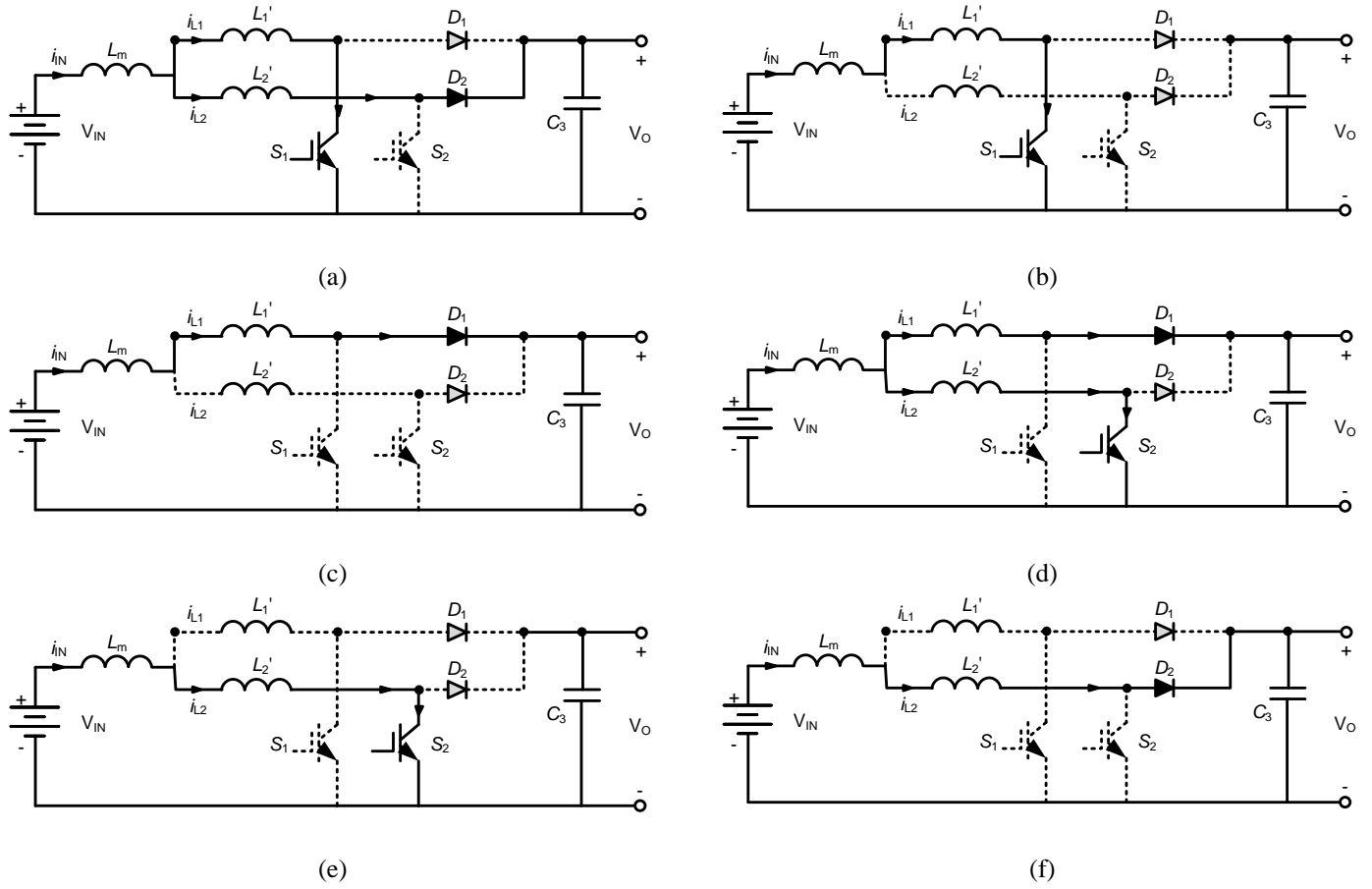


Figure 4. Equivalent circuits during the switching states of the interleaved boost converter.

The converter operation is explained for each switching state as follows:

**Interval  $t_0 - t_1$ , Figure 4(a)**

At time  $t_0$ , it's assumed that the remaining power in  $L_2'$  acquired in the previous switching cycle.  $D_2$  is assumed *on* during this state. At time  $t_0$  the switch  $S_1$  is closed, then the current in the inductor  $L_1'$  begins to rise while the current in  $L_2'$  drops with a rate of change given by:

$$\frac{di_{L_2}}{dt} = \frac{-V_o}{L_1' + L_2'} \quad (4)$$

**Interval  $t_1 - t_2$ , Figure 4(b)**

At time  $t_1$ ,  $i_{L_2}$  drops to zero while that  $i_{L_1}$  continues rising with a rate of change,

$$\frac{di_{L1}}{dt} = \frac{V_{IN}}{L'_1 + L_m} \quad (5)$$

**Interval  $t_2 - t_3$ , Figure 4(c)**

At  $t_2$ ,  $S_1$  opens. The energy stored in the inductor  $L_1$  is transferred to the output capacitor through  $D_1$ .  $i_{L1}$  current begins to decrease with a rate change determined by (6):

$$\frac{di_{L1}}{dt} = \frac{-(V_o - V_{INPUT})}{L_1} \quad (6)$$

**Interval  $t_3 - t_4$ , Figure 4(d)**

In this interval,  $S_2$  is closed at  $t_3$ . The current in the inductor  $L'_2$  begins to increase, while  $L'_1$  continues to discharge with a rate of change given by (7):

$$\frac{di_{L1}}{dt} = \frac{-V_o}{L'_1 + L'_2} \quad (7)$$

**Interval  $t_4 - t_5$ , Figure 4(e)**

At time  $t_4$ , the current  $i_{L1}$  reaches zero while  $i_{L2}$  continues to increase with a rate given by (8):

$$\frac{di_{L2}}{dt} = \frac{V_{INPUT}}{L'_2 + L_m} \quad (8)$$

**Interval  $t_5 - t_6$ , Figure 4(f)**

At  $t_5$ ,  $S_2$  opens and the inductor  $L'_2$  begins to discharge. The discharge reason in  $i_{L'_2}$  is expressed by (9):

$$\frac{di_{L2}}{dt} = \frac{-(V_o - V_{INPUT})}{L_2} \quad (9)$$

Figure 5 shows the main waveforms of the interleaved boost converter.

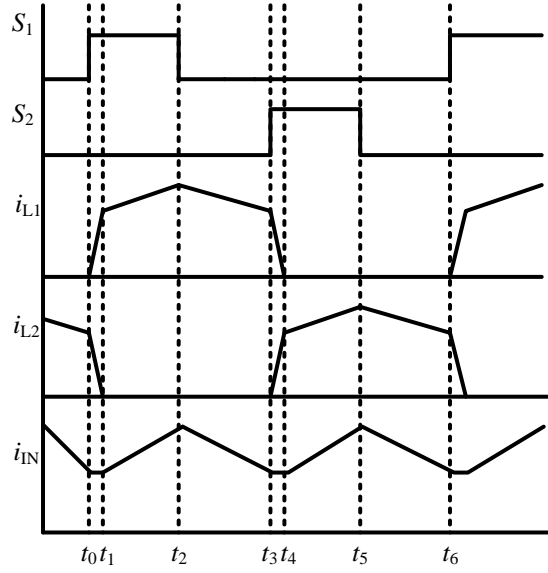


Figure 5. Main waveforms of the Interleaved boost converter.

In order to get the output voltage relationship, it is assumed that converter's power losses are negligible. Hence, the output power  $P_o$  is equal to the input power  $P_i$ , as is established by:

$$P_i = P_o \quad (10)$$

$$V_i(I_1 + I_2) = \frac{V_o^2}{R_L} \quad (11)$$

It is also assumed that,

$$D_1 = D \quad (12)$$

$$D_2 = D + \Delta D \quad (13)$$

$$L_1 = L_2 = L \quad (14)$$

In this way the output voltage is given by (15).

$$V_o = \frac{[1+2(1-k)(0.5+D)(A)] + \sqrt{[1+2(1-k)(0.5+D)(A)]^2 - 4(1-k)(1-\Delta D)\left[\frac{4L(1-k)}{R_L T}\right] + A}}{2\left[\frac{4L(1-k)}{R_L T} + A\right]} V_{IN} \quad (15)$$

where:

$$A = 1 - 2D - \Delta D \quad (16)$$

## 2.2 Output converter.

The basic operating principle of multilevel converter depends on the conduction states of the switches  $S_1$  and  $S_2$  of the input stage. Basically, it involves the transfer of energy to the capacitor  $C_4$  through the capacitors  $C_1$  and  $C_2$ . The output voltage is doubled due to the sum of the voltages of the capacitors  $C_3$  and  $C_4$ .

When  $S_1$  is on, the capacitor  $C_1$  is charged to the voltage of  $C_3$ , at the intervals  $t_0 - t_1$  and  $t_1 - t_2$  thus, neglecting the voltage drop of the diode  $D_3$  results in:

$$v_{C1} = v_{C3} \quad (17)$$

Figure 6 shows the converter configuration that allows charging  $C_1$  from  $C_3$ .

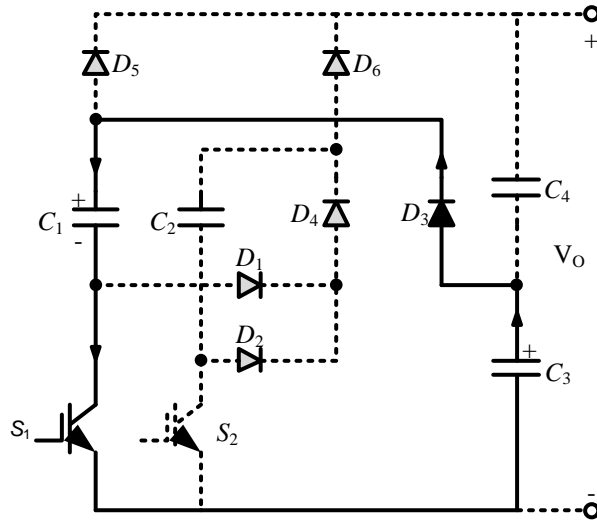


Figure 6. Charging process of capacitor  $C_1$ .

Similarly, during intervals  $t_3 - t_4$  and  $t_4 - t_5$ , when  $S_2$  is on, the capacitor  $C_2$  is charged to the output voltage of the interleaved boost converter through  $C_3$ , Figure 7.



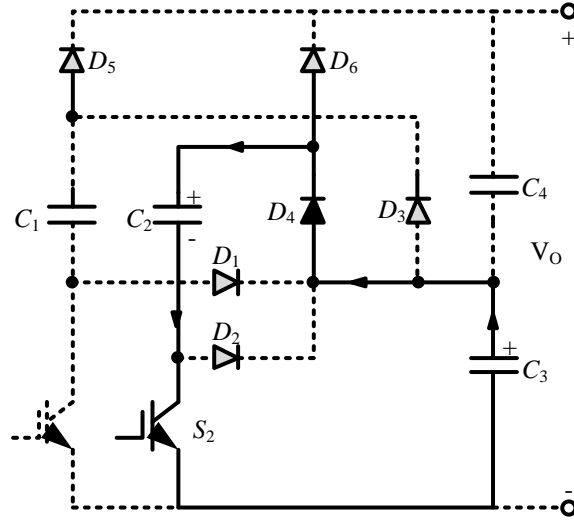


Figure7. Charging process of capacitor  $C_2$ .

Neglecting the voltage drop in  $D_4$ , the voltage in  $C_2$  is determined by,

$$v_{C2} = v_{C3} \quad (18)$$

The capacitor  $C_4$  is charged during the time intervals while inductors  $L_1$  y  $L_2$  are discharging due to  $S_1$  or  $S_2$  are *off*, respectively.

## 2.2 Multilevel-Interleaved boost converter.

The proposed converter integrates the interleaved boost converter and the multilevel converter in order to get a high-gain converter. The output voltage is the sum of capacitors' voltage  $C_3$  and  $C_4$ . Figure 8 illustrates the capacitor's  $C_4$  charging process, when  $L_1$  y  $L_2$  are discharging.

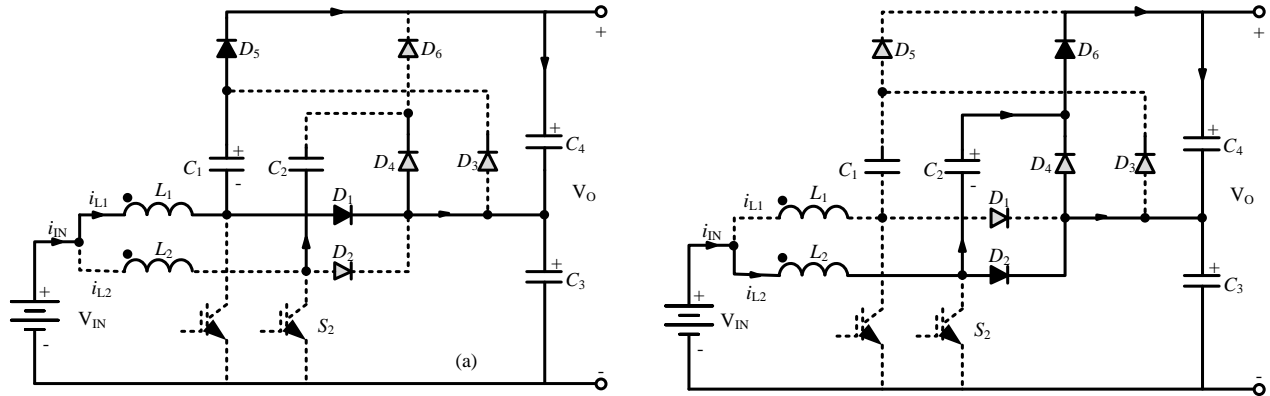


Figure 8. Charging process of the capacitor  $C_4$  since  $L_1$ . (b) Charging process of  $C_4$  since  $L_2$ .

The output voltage of the multilevel-interleaved boost converter is the result of to multiply the output voltage of the interleaved boost converter  $n$  times the output voltage of the multilevel converter:

$$V_{IN} = 2 * v_o \quad (19)$$

The advantage of the multilevel converter is the possibility to add levels in order to increase the output voltage.

Figure 9 shows the gain of the proposed converter. It is noteworthy that the multilevel-interleaved boost converter gain is almost twice the gain of a conventional boost converter operating in Continuous Conduction Mode (CCM), for the same duty cycle.

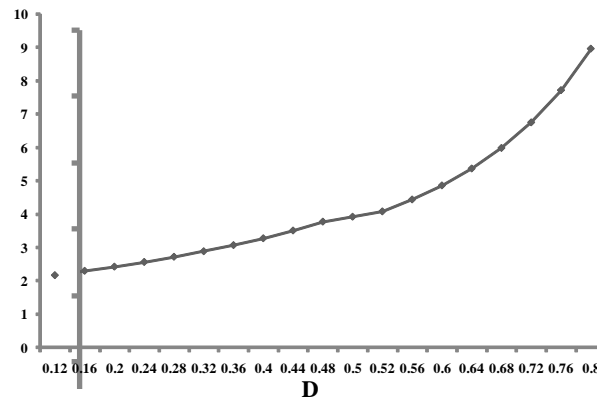


Figure 9. Estimated gain of the proposed converter

The estimated efficiency of the proposed converter, Figure 10, has been evaluated through co-simulation, where an inductor resistance of 10 mΩ and on-resistance of 50 mΩ in the switches were taken into account.

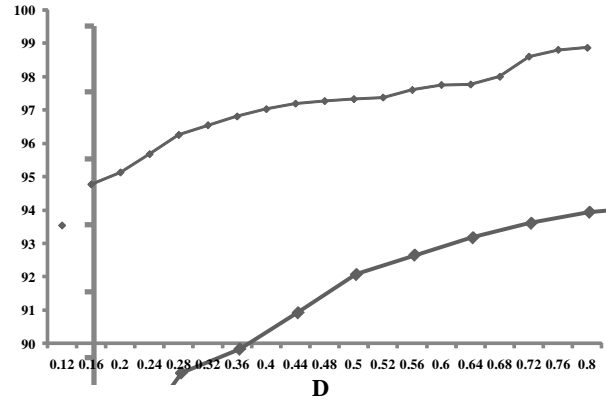


Figure 10. Estimated efficiency of the proposed converter.

A comparison of the proposed converter respect to a conventional boost converter is illustrated in Table 1.

Table B.I Comparison of the characteristics between the proposed converter and a conventional boost converter

	Conventional boost converter in CCM	Proposed converter
RMS current in input inductor	Normalized to 1 (1 winding)	0.707 (2 windings)
Ripple in the output voltage	Large	Small
Number of switches	1	2
Number of diodes	1	6
Average current in the switches	Normalized to 1	0.5
Average current in the diodes	Normalized to 1	0.5
Gain	Normalized to 1	≈ 2

### 2.3 Design example.

In this section, a 250 W prototype is designed. Assuming an input voltage of 30 VDC and assuming that the application requires an output voltage of 120 VDC, a gain voltage of 4 is required. Therefore, if the multilevel gain voltage is 2, then the interleaved boost converter gain must be 2.

Since interleaved boost converter operation is similar to that of the conventional boost converter, assuming a duty cycle of 50 %, the inductance value for the input inductors becomes:

$$L_1 = L_2 = \frac{D \cdot V_{OUTPUT}}{2 \cdot f_{sw} \cdot \Delta I} \quad (20)$$

where  $f_{sw}$  is the switching frequency and  $\Delta I$  is the current ripple in the input inductors. Assuming a 10 % of current ripple to full load, the inductance values become  $L_1 = L_2 = 75 \mu H$ .

The capacitance is calculated by,

$$C = \frac{I_{INPUT} * (1-D) * D}{f_{sw} * \Delta v_{OUTPUT}} \quad (21)$$

where  $I_{INPUT}$  is the average input current and  $\Delta V_{OUTPUT}$  is the output voltage ripple. Thus, assuming a voltage ripple minor than 1 % of the nominal output voltage, the capacitance obtained is 20  $\mu F$ .

### 3. Results and discussions.

Results of co-simulation of the 250 W prototype designed are exposed in this section. The proposed converter was simulated in Multisim®, for the power stage simulation, and Labview® for the control stage. Ideal diodes and switches with an on-resistance of 50 m $\Omega$  are utilized. Power converter parameters are shown in Table 2.

Table 2. Converter's Parameters

Parameter	
Input voltage ( $V_{INPUT}$ )	30 VCD
Input inductor ( $L = L_1 = L_2$ )	75 $\mu H$
Coupling factor ( $k$ )	0.95
Capacitances, $C_1 = C_2 = C_3 = C_4$	20 $\mu F$
Load ( $R_L$ )	57.6 $\Omega$
Switching frequency ( $f_{sw}$ )	100 kHz

Figure 11 shows the co-simulation results for the case when the duty cycle for  $S_1$  and  $S_2$  are identical ( $D = D_1 = D_2 = 0.25$ ).

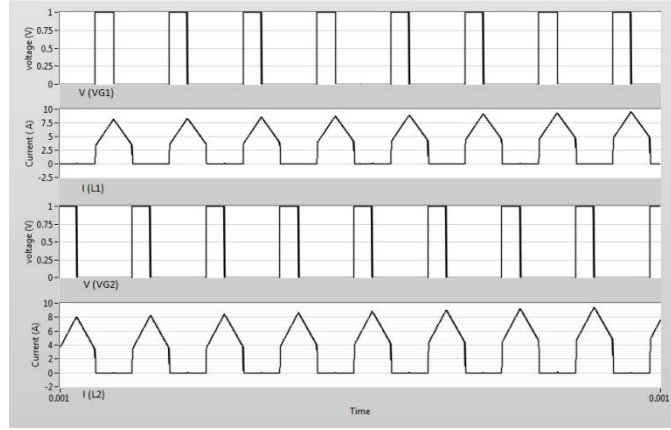


Figure 11. Co-simulation results of the proposed converter. From top to down: gate signal for  $S_1$ , current waveform in  $L_1$ , gate signal on  $S_2$ , and current waveform in  $L_2$ .

The waveforms of Figure 11 show that the input current is distributed uniformly between each phase. Furthermore, while each one of the phases operates in MCD ( $i_{L1}$ ,  $i_{L2}$ ), the current taken from the FC is a continuous waveform, with two times the switching frequency  $f_{sw}$  of the switches  $S_1$  and  $S_2$ . Moreover, the ripple of the input current in the converter proposed is maintained within the design range.

Figure 12 shows the output voltage for the case where the duty cycles of  $S_1$  and  $S_2$  are equal to 0.25.

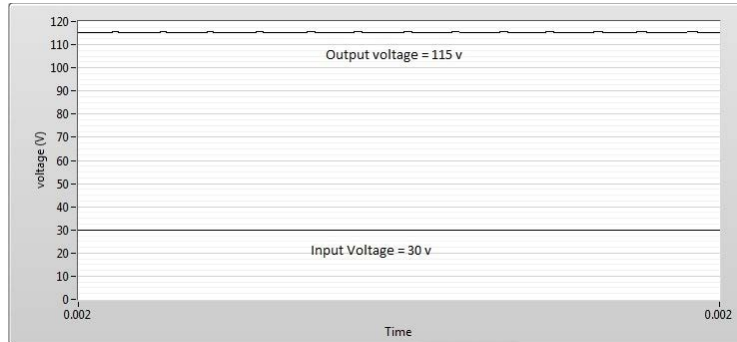


Figure 12. Output and input voltage of the multilevel-interleaved boost converter.

As shown in Figure 12, the gain of the output voltage is almost four times the input voltage. The gain in a boost converter with a single stage work cycle of 0.25 would theoretically be 1.33. This demonstrates that the proposed converter has a gain greater than the boost converter of a single stage.

#### **4. Conclusions**

In this paper we have presented a new topology of boost converter for fuel cell applications. The main advantages of the converter proposed are:

- Low ripple in the current that is demanded to the fuel cell.
- High gain of the output voltage of the converter.
- Uniform distribution of the input current between the converter phases, despite of variations on its duty cycles.
- No current sensors or current control loop are required in order to maintain the equal current sharing between the phases of the power converter
- It is feasible to increase the levels of the multilevel converter in order to increase the gain of the output voltage.

#### **5. Acknowledgments**

The authors wish to thank to PROMEP for the support for this project under grant UQROO-EXB-072

#### **6. References**

- [1] L. Palma, M.H. Todorovic and P. Enjeti , “A high gain transformer-less DC-DC converter for fuel cell applications”, *Proc. IEEE Power Electronics Specialists Conference*, Jun. 2005, pp. 2514.
- [2] G. Fontes, C. Turpin, R. Saisset, T. Meynard and S. Astier, “Interactions between fuel cells and power converters influence of current harmonics on a fuel cell stack”, *Proc. IEEE Power Electronics Specialists Conference*, Jun. 2004, pp. 4729.
- [3] O. García, P. Zumel, A. de Castro, J.A. Cobos, “Automotive DC-DC bidirectional converter made with many interleaved buck stages”, *IEEE Transactions on Power Electronics*, vol. 22, no. 4, pp. 578, July 2007.
- [4] J.C. Rosas-Caro, J.M. Ramirez, F.Z. Peng and A. Valderrabano, “A DC-DC multilevel boost converter”, *Power Electronics IET*, vol. 3, no. 1, pp. 129, January 2010.
- [5] P.W. Lee, Y.S. Lee, K.W. Cheng, X.C. Liu, “Steady-state analysis of an interleaved boost converter with coupled inductors”, *IEEE Transactions on Industrial Electronics*, vol. 47, no. 4, pp. 578, August 2000.